haematologica
Journal of the Ferrata Storti Foundation

Homeostatic imbalance between von Willebrand factor and ADAMTS13 in hemorrhagic shock-induced endotheliopathy

by Yi Wang, Sarah Abdullah, Feng Wu, Katie Houck, Roumen Vesselinov, Xiaoyun Fu, Lin Zou, Myung Park, Jing-Fei Dong and Rosemary Kozar

Received: June 4, 2026.
Accepted: August 21, 2026.

Citation: Yi Wang, Sarah Abdullah, Feng Wu, Katie Houck, Roumen Vesselinov, Xiaoyun Fu, Lin Zou, Myung Park, Jing-Fei Dong and Rosemary Kozar. Homeostatic imbalance between von Willebrand factor and ADAMTS13 on hemorrhagic shock-induced endotheliopathy.
Haematologica. 2026 Sept 3. doi: 10.3324/haematol.2026.301364 [Epub ahead of print]

Homeostatic imbalance between von Willebrand factor and ADAMTS13 in hemorrhagic shock-induced endotheliopathy

Yi Wang[1], Sarah Abdullah[2], Feng Wu[2], Katie Houck[1], Roumen Vesselinov[2], Xiaoyun Fu[1,3], Lin Zou[2,4], Myung Park[5], Jing-Fei Dong[1,3], Rosemary Kozar[2,6]

[1]Bloodworks Research Institute, Seattle, WA, USA

[2]Shock Trauma and Anesthesiology Research (STAR) Center, University of Maryland School of Medicine; Baltimore, MD, USA.

[3]Division of Hematology and Oncology, Department of Medicine, University of Washington School of Medicine, Seattle, WA

[4]Translational Research Program, Department of Anesthesiology, University of Maryland School of Medicine; Baltimore, MD, USA

[5]Department of Surgery, Mayo Clinic College of Medicine, Rochester, MN

[6]Shock Trauma Center, University of Maryland School of Medicine, Baltimore, MD, USA

Corresponding Author:

Rosemary Kozar

22 S Green St. T1R40

Baltimore, MD 20210

410-328-3495 phone 410-328-6382 fax

rkozar@som.umaryland.edu

Short title: Imbalance of VWF and ADAMTS13 in Endotheliopathy

Data Sharing Statement: For original data please contact Rosemary Kozar (rkozar@som.umaryland.edu)

Acknowledgments: The authors would like to thank Bloodworks Mass Spectrometry Core facilities for their assistance.

Author contributions: RAK and JFD conceived the research study, analyzed the data and wrote the manuscript with input and approval from all authors. YW and XYF designed and performed mass spectrometry experiments to measure VWF cleavage and oxidation. LZ assisted with Luminex design and interpretation; SA acquired human data and conducted human Luminex experiments; MP critically analyzed results and reviewed manuscript, FW conducted animal experiments and analyzed animal data; RV performed the statistical analysis including CART modeling; KLH performed partial data analysis.

Conflicts of interest: The authors declare no competing financial interests.

Funding This work was supported by NIH R01GM140983 to RAK and JFD. SA was supported by NIH T32HL007698.

Supplementary file: Methods, one tables, six figures

ABSTRACT

Endothelial dysfunction in patients after severe injury with hemorrhagic shock is associated with excessive release of ultralarge von Willebrand factor (VWF) without a corresponding increase in ADAMTS13 (A disintegrin and metalloprotease thrombospondin type 1 motifs, member 13), resulting in acquired ADAMTS13 deficiency and VWF hyperadhesive activity. We hypothesized that the VWF to ADAMTS13 imbalance is exacerbated by increased VWF oxidation, rendering it resistant to cleavage by ADAMTS13. Plasma indices of endotheliopathy and coagulopathy in 100 hemorrhagic shock patients were obtained, ADAMTS13-to-VWF ratio was calculated and correlated with indices of adverse outcomes using Classification and Regression Tree modeling. A novel mass spectrometry method was used to quantify the rate of VWF cleavage in individual patients. In a mouse model of polytrauma and hemorrhagic shock, a single dose of human recombinant ADAMTS13 was administered and VWF cleavage, VWF activity, and parameters of lung dysfunction examined. We detected a reduced rate of cleavage and increased oxidation rate of selective methionine residues of VWF in these patients. In mice, recombinant ADAMTS13 decreased the adhesive activity and enhanced cleavage of plasma VWF, and improved parameters of lung dysfunction. The present study supports the conclusion that an imbalance between VWF and ADAMTS13 drives, at least in part, the endotheliopathy of trauma and the associated adverse outcomes and suggests a potential therapeutic target for severely injured patients with hemorrhagic shock.

Introduction

Hemorrhagic shock (HS) remains a major cause of mortality after severe injury (1). In survivors, dysregulation of endothelial cells, especially in the microvasculature, contributes to secondary coagulopathy, multiple organ failure, and death (2). Recent studies suggest that von Willebrand factor (VWF) plays a major role in trauma-induced injury to endothelial cells (3-6), which are the primary cells of VWF synthesis. Newly synthesized VWF monomers first dimerize and then multimerize to form large multimers of variable sizes (7, 8). After synthesis, VWF multimers are either constitutively released into the circulation or stored in Weibel-Palade bodies of endothelial cells and the α-granules of megakaryocytes and platelets, where multimerization continues (9, 10) to form ultralarge VWF multimers (ULVWF). These ULVWF multimers are released rapidly from endothelial cells into circulation upon endothelial injury by traumatic, ischemic, and inflammatory stimuli (11-13), as demonstrated by the loss of the protective endothelial glycocalyx (14, 15). The ULVWF multimers are intrinsically hyperadhesive and can spontaneously bind to and activate platelets and endothelial cells (7, 10, 16, 17), whereas smaller VWF multimers in plasma during homeostasis only bind platelets when they are immobilized onto the subendothelial matrix exposed at the site of vascular injury (10, 16, 17). Once endothelial cells are injured and lose syndecan-1/glycocalyx, ULVWF multimers can anchor to endothelial cells to form string-like structures (14, 15, 18, 19), which tether and activate platelets and leukocytes to cause vascular inflammation and microvascular thrombosis (18, 20). These ULVWF strings are rapidly cleaved by ADAMTS13 (A disintegrin and metalloprotease thrombospondin type 1 motifs, member 13) and released from the endothelial surface to become smaller VWF multimers found in plasma during homeostasis (17, 21, 22). The cleavage prevents spontaneous VWF-platelet thrombosis while maintaining hemostasis. However, severe trauma

could reduce the rate of VWF cleavage because of the increased release of ULVWF (11-13, 23) without a corresponding increase in ADAMTS13, leading to an acquired ADAMTS13 deficiency.

We hypothesized that traumatic HS patients would have elevated plasma indices related to inflammation, endotheliopathy, and coagulopathy, and in particular, VWF hyperadhesive activity due to a decreased ADAMTS13-to-VWF ratio. We therefore measured representative variables and analyzed them through Classification and Regression Tree (CART) machine learning to identify no risk and high risk patient cohorts for multiple organ failure and death. We further hypothesized that traumatic HS patients develop an imbalance between ADAMTS13 and VWF and increased VWF oxidation, leading to acquired ADAMTS13 deficiency and VWF hyperadhesive activity. To address this hypothesis, we quantified VWF cleavage in patient plasma using a mass spectrometry based proteomic assay and evaluated methionine oxidation of VWF and the overall levels of plasma oxidative stress. Lastly, we used a mouse model of polytrauma and HS to determine the potential therapeutic benefit of recombinant ADAMTS13 to reduce the levels of endotheliopathy and coagulopathy.

METHODS

Detailed methods in the supplemental file.

Human Study

Patients were recruited between 7/5/2022 and 1/24/2024 at the Shock Trauma Center at the University of Maryland School of Medicine after Institutional Review Board approval (HP-00097837).

Patient cohort and sample collection.

Inclusion criteria are shown in **Supplementary Figure 1**. Samples were obtained upon arrival prior to blood transfusion, and in a smaller cohort of patients, post resuscitation (no blood transfusion for at least one hour) (24), and at 24 hours. Age and sex matched minimally injured (MI) patients were used as clinically relevant controls (14). A subcohort of ICU patients was recently reported (25).

Demographics, injury severity scores (ISS), laboratory values, and clinical endpoints and outcomes, including mortality, multiple organ failure (MOF), and sequential organ failure assessment (SOFA) scores were collected. MOF was considered as present with a score of ≥ 3 (26).

Plasma biomarkers

IL-6, syndecan-1, angiopoietin 1 and 2, tissue factor, thrombomodulin, VWF-A2, and ADAMTS13 were measured using a multiplex immunoassay (Luminex Discovery Assay, R&D) and quantified using MAGPIX, Luminex 100/200 laser sorting and detection platforms.

ADAMTS13 cleavage of VWF in humans and mice

We have previously developed a mass spectrometry-based assay to simultaneously quantify the rate of VWF cleavage and degree of methionine (Met) oxidation in plasma from individual trauma patients (27, 28, 29). This MS method was also modified to quantify mouse VWF cleavage rate because the sequence of tryptic peptide of mouse VWF produced by ADAMTS13 differs from that of human VWF (**Supplemental Figure 2**).

Animal study

The Animal Care and Use Committee of Institutes at the University of Maryland School of Medicine approved the protocol (IACUC 0818008). To mimic human trauma, a mouse model of

polytrauma and HS was used (Supplemental Method), as we previously reported (30). At the end of HS, recombinant human ADAMTS13 (rhADAMTS13 (5)) was randomly administered at 10 μg/mouse (or vehicle for controls) followed by hypotensive resuscitation. Mice were then euthanized by exsanguination under isoflurane and lungs and blood harvested; n= 10/group (31). Total protein was measured in alveolar fluid and lung histopathologic injury and microvascular thrombi detected.

Statistics

Mean and standard deviation is presented for normally distributed data and median and interquartile range if normality was not met. Analysis of Variance (ANOVA) was utilized for data that conformed to a normal distribution, and non-parametric tests were used when the assumption was violated. The non-parametric analysis included Spearman correlation and Kruskal-Wallis tests. Chi-square test was used for determining the relationship between two categorical variables with a significant level of 5% ($p<0.05$).

Classification and Regression Tree (CART) machine learning model were utilized (32). All available variables were included in the pool of explanatory variables for the CART model. The final model included only the four variables presented on the tree. CART also provides Variable Importance Measures (VIM), of which the most important factor has a score of 100, followed by the next important factors with lower scores.

RESULTS

Hemorrhagic shock cohort

Patients were primarily young adults, male, with a blunt mechanism, and per our inclusion criteria, all were hypotensive (**Table 1**). This severely injured cohort (ISS 22 [6, 33]) had a

prolonged ICU stay of 11.8 [6.3, 26.2] days and were at high risk for adverse outcomes with 24 % developing either MOF or death. The minimally injured (MI) were age- and sex-matched patients as clinically relevant controls (n= 39; median ISS 1 [1, 2]): MI cohort age 42 [28, 54] vs HS 39 [31, 53; p=0.8] and MI cohort male 82% vs HS 81% (p=0.9).

We quantified IL-6 as a measure of inflammation, syndecan-1, angiopoietin-1, and angiopoietin-2 as measures of endothelial cell activation/injury, and tissue factor and thrombomodulin as measures of coagulopathy. All indices were significantly elevated ($p< 0.001$) in HS patients compared to MI patients (**Figure 1**). We also measured ADAMTS13 and VWF and calculated their ratio to indicate an acquired ADAMTS13 deficiency state due to significantly elevated VWF-A2 without a parallel increase of ADAMTS13 (**Figure 2A-C).**

We then examined the potential correlations between these indices and other parameters of endothelial dysfunction. There was a positive correlation between levels of plasma syndecan-1 and VWF ($r=0.375$, $p<0.001$), between syndecan-1 and ADAMTS13 ($r=0.315$, $p=0.002$), and as between IL-6 and VWF ($r=0.343$, $p<0.001$). When analyzing only patients who received at least 8 units of blood products as a more severely injured at risk cohort, additional correlations were noted, most notably between VWF and ADAMTS13 and syndecan-1 and ADAMTS13, as well as the indices of coagulopathy and clinical outcomes (**Table 2 and Figures 2D and 2E**). **Figure 2F** shows the significant correlation between VWF-A2 and ADAMTS13 (rho 0.558, $p<0.0001$) in these high transfusion patients. Additionally, ADAMTS13 and VWF were significantly correlated to SOFA scores on day 1 (ADAMTS13; rho 0.463, $p=0.001$ and VWF; rho 0.371, $p=0.001$) while ADAMTS13 was also significantly correlated to SOFA scores on day 4 (rho 0.323, $p=0.029$) and with ventilator days (rho 0.360, $p=0.014$).

We next used Classification and Regression Tree (CART) modeling to uncover groups of patients based on combined factors of measured analytes to determine risk levels of adverse outcomes, defined as either MOF or death, which was found in 24% of our patient cohort. Six different groups or "terminal nodes" were identified by CART as having extreme values of outcomes (**Figure 3)**. Four groups of patients had no adverse outcomes. Three of the four groups had a low syndecan-1 (defined as < 81.9 ng/ml): low syndecan and high angiopoietin 2 (defined as > 32.6 ng/ml); low syndecan-1, low angiopoietin 2 (defined as < 32.6 ng/ml), and low tissue factor (defined as < 42.5 pg/ml); low syndecan-1, low angiopoietin 2, high tissue factor (defined as > 42.5 pg/ml), and high ADAMTS13 (defined as > 0.98 μg/ml). The fourth no risk group had a high syndecan-1 > 81.9 ng/ml but a lower tissue factor < 58.6 pg/ml. Interestingly the high-risk group of 46.7% was identified with a low syndecan-1, low angiopoietin 2, but a high tissue factor and a low ADAMTS13, while the highest risk group of 70.8% had a high syndecan-1 > and the highest tissue factor >58.6 pg/ml.

The CART model had a very good predictive ability with an AUROC=0.92 for the training data and an AUROC=0.71 for the validation data. CART also provides variable important measures (VIMs) to rank the factors in the CART tree, in which the most important factor has a score of 100, with each additional factor listed in decreasing importance (**Table 3**). Plasma levels of VWF-A2 and ADAMTS13 were among the top 10 VIMs.

VWF cleavage and oxidation

We randomly selected ten longitudinal samples from the patients collected at three time points (admission, post-resuscitation, and 24 hours) with available samples from the larger cohort of 100 patients for measuring VWF cleavage and methionine oxidation. Patients in the longitudinal

cohort were age and sex matched with comparable arrival blood pressure and lactate to the larger cohort (**Table 1**). We first confirmed that this subpopulation of patients had similar profiles of measured analytes between MI and HS patients and then examined changes of these analytes over time. IL-6, syndecan-1, angiopoietin-2, tissue factor, and thrombomodulin all remained significantly ($p<0.001$) elevated from admission to 24 hours (**Supplementary Figure 3**). Angiopoietin-2 and thrombomodulin were in fact maximally increased at 24 hours post resuscitation. There was also a similar significant ($p<0.001$) increase in VWF-A2 in HS subcohort, while ADAMTS13 was not increased in either MI or HS subcohorts. To ensure that the acute stress of trauma in the MI patients was not influencing VWF-A2 or ADAMTS13, we compared results to healthy donor plasma: VWF-A2 in healthy donors was 5.01 ng/ml (4.67, 8.12) compared to MI 4.77 ng/ml (2.47, 8.59, $p = 0.887$), whereas ADAMTS13 in healthy donors were 1.33 ug/ml (1.06, 1.38) as compared to MI at 0.96 ug/ml (0.66, 1,25, $p=0.368$)**.**

VWF-Ag significantly decreased at post-resuscitation compared to admission ($p<0.01$) and further decreased at 24 hrs ($p<0.05$). VWF-A2 showed a similar progressive decrease over time at both post resuscitation ($p<0.001$) and 24 hours ($p<0.001$). In contrast, ADAMTS13 remained unchanged in samples collected at these timepoints (**Supplemental Figure 4**), resulting in a significantly reduced ADAMTS13-to-VWF-A2 ratio ($p<0.05$) at admission followed by gradual increase through 24 hours ($p<0.001$, **Figure 4A**). An important note was that patients received ADAMTS13 containing blood products including whole blood or FFP 4.5 [2.3, 7.8] units through 24 hours which did not increase their plasma of ADAMTS13 levels.

By measuring VWF-Ag, which detected all VWF, and VWF-A2, which detected primarily active VWF, we determined that the active VWF accounted for approximately 26% ± 11% of total plasma VWF in samples collected upon admission. The percent of active VWF gradually

reduced in samples collected thereafter. This increase in active VWF was further validated by enhanced VWF binding to collagen (VWF:CB, **Figure 4B;** $p<0.001$), elevated ratio of VWF:CB to VWF-Ag (**Figure 4C;** $p<0.001$), and higher levels of platelet-derived and VWF bound extracellular vesicles ($CD41^+/VWF^+$ pEVs, **Figure 4D;** $p<0.001$) in HS patients, compared to those of MI patients. The levels of VWF^+ pEVs served as a surrogate marker for VWF-induced platelet activation.

Consistent with increasing VWF adhesive activity, the MS detected significantly reduced ($p<0.05$) VWF cleavage by ADAMTS13 in plasma samples collected at post resuscitation and 24 hours (**Figure 4E**). The MS results also showed significantly ($p<0.05$) increased levels of plasma oxidative stress, defined by protein-bound Cysteines (protein-ss-Cys) (33) in samples collected at all three timepoints (**Figure 4F**). Consistent with increasing oxidative stress, we also detected oxidation of all seven methionine residues in the A1-A3 domains of VWF from patients with severe trauma compared to MI patients. Met^{1303} ($p=0.016$), Met^{1385} ($p=0.037$) and Met^{1761} ($p<0.05$) were significantly increased while the differences in Met^{1304}, Met^{1521}, Met^{1860} and Met^{1606} did not reach statistical significance (Supplementary **Table 1**). The Met^{1606} forms the peptide bond of Tye^{1605}-Met^{1606} that is cleaved by ADAMTS13 and its oxidation induced *in vitro* renders VWF resistant to cleavage by ADAMTS13 (29). Among longitudinally collected samples, Met^{1606} was not oxidized in plasma samples collected at 24 hours post injury (**Supplementary Table 1**). Nonetheless, linear regression analysis showed that VWF cleavage levels at 24 hours were highly correlated with the level of protein-ss-Cys ($R2 = 0.730$, $p<0.001$).

ADAMTS13 as a potential therapeutic in mice with polytrauma and HS

To determine if augmentation of ADAMTS13 would reduce the hyperadhesive activity of VWF and mitigate the detrimental effects of HS, rhADAMTS13, which cleaves mouse VWF (34), was

tested in a clinically relevant mouse model of polytrauma and HS. Polytrauma HS mice developed acute lung injury defined by a significant increase in histopathologic injury ($p<0.001$, **Figure 5A**), significantly higher levels of bronchoalveolar proteins ($p<0.001$, **Figure 5B**) and extensive microthrombi ($p<0.001$, **Figure 5C**) compared to sham mice. Consistent with the results of injured patients with HS, trauma-HS mice also had significantly higher levels of VWF-Ag ($p<0.001$, **Figure 5D),** VWF:CB ($p<0.001$, **Figure 5E**), and VWF:CB to VWF-Ag ratio ($p<0.001$, **Figure 5F**), indicating that VWF in these mice was intrinsically hyperadhesive. This observed VWF hyperadhesive activity is further supported by high levels VWF^+ platelet EVs ($CD41^+$) in trauma-HS mice ($p<0.001$, **Figure 5G**). Importantly, acute lung injury, microvascular thrombosis and VWF hyperadhesive activity were all significantly ($p<0.001$) reduced in the trauma-HS mice that received a single bolus dose of rhADAMTS13 (**Figure 5A-5G**).

To further investigate whether reduced VWF hyperactivity and acute lung injury in trauma-HS mice receiving rhADAMTS13 was attributable to increased VWF cleavage, we modified the MS method to quantify the rate of cleaving mouse VWF by ADAMTS13. Consistent with the findings in trauma patients, VWF cleavage was significantly lower in trauma-HS mice than sham mice ($p<0.001$) and the reduction was reversed in mice receiving a single bolus infusion of rhADAMTS13 to the level comparable to sham mice ($p<0.001$, **Figure 5H**).

DISCUSSION

Following trauma, the endothelium serves as the site for not only initiating hemostasis but also for propagating inflammation, endothelial injury/loss of glycocalyx, and coagulopathy, resulting in the “endotheliopathy of trauma (EOT)”. EOT is associated with mortality and adverse

outcomes (2, 35). The role of VWF after traumatic injury has been increasingly recognized (36-40). In the current study, to address our initial hypothesis that HS patients would have elevated plasma indices related to inflammation, endotheliopathy, and coagulopathy, we used Luminex to confirm this hypothesis. Using this information, we next used CART machine learning to identify four no risk and two high risk patient cohorts who developed multiple organ failure or death. Finding a positive correlation between VWF and related variables for inflammation, endotheliopathy, and coagulopathy led us to also hypothesize that HS patients develop an imbalance between ADAMTS13 and VWF and increased VWF oxidation, leading to acquired ADAMTS13 deficiency and VWF hyperadhesive activity. To therefore quantified VWF cleavage in patient plasma using a mass spectrometry based proteomic assay This assay allowed us to quantify simultaneously VWF cleavage and methionine oxidation of individual patients. The latter has been shown to make VWF resistant to ADAMTS13 cleavage (29). Lastly, using a mouse model of polytrauma and HS, we found that these mice had intrinsically hyperadhesive VWF, consistent with the results of injured patients with HS. Additionally, acute lung injury, microvascular thrombosis and VWF hyperadhesive activity were all significantly reduced in the trauma-HS mice that received a single bolus dose of rhADAMTS13

We demonstrated a ADAMTS13 -VWF imbalance caused by excessive VWF release without a parallel increase in ADAMTS13, resulting in insufficient VWF cleavage. We quantified VWF cleavage using a more accurate and quantitative MS method to address the limitations of conventional assays, which measure either the reduction of VWF molecular size or proteolytic fragments of cleaved VWF using immunoblots or the cleavage rate of a recombinant VWF-A2 peptide by patient plasma. The former is semi-quantitative, whereas the latter does not measure the actual cleavage of endogenous VWF in trauma patients.

We also found that methionine residues in the A1-A3 domains of VWF are oxidized at higher levels in patients with severe trauma compared to MI patients, even though some did not reach statistical significance due to a small sample size. These results raise the possibility that VWF becomes active during the early stages of severe trauma shock by undergoing oxidation-dependent conformational changes. This possibility is supported by the finding that these patients had higher levels of intrinsically active VWF, defined by a high VWF-A2-to-VWF-Ag ratio. This finding is important because circulating VWF is maintained in an inactive state during homeostasis through the formation of a complex between the A1 and A2 domains to prevent VWF from binding platelets and being cleaved by ADAMTS13 (41, 42). This complex is formed when the two vicinal cysteine residues in the A2 domain are in a reduced state (i.e., as free thiols) but is disrupted when these cysteine residues are oxidized to form a disulfide bond (43). Consistent with this notion, we detected elevated levels of protein-bound (oxidized) cysteines in patient samples. Furthermore, these HS patients also had enhanced methionine oxidation of VWF. Methionine residues are often hidden in the hydrophobic core but become more polar and hydrophilic when oxidized, resulting in conformational changes in VWF. Our findings suggest that measuring levels of A2-exposed VWF is more significant than total VWF antigen for detecting conformationally activated (VWF-A2 exposed) VWF. VWF oxidation and its impact on VWF activity are schematically shown in **Supplemental Figure 5.**

The imbalance between VWF and ADAMTS13 we detected support early reports in both severely injured adult and pediatric patients (37, 38) and in mouse models of traumatic brain injury (5, 6). In the patient studies, low ADAMTS13 levels were correlated with coagulopathy, similar to the current study in patients with higher blood product requirements. An important finding is that blood product-based resuscitation did not increase ADAMTS13 antigen,

suggesting an ongoing deficiency or consumption of the metalloprotease. It is plausible that this is related to ongoing oxidative stress due to resuscitation-related reperfusion injury, which may be an unidentified yet potentially modifiable factor.

We used CART analysis to investigate which parameters contribute to adverse outcomes defined as death or MOF, and identified ADAMTS13, syndecan-1, angiopoietin-2, and tissue factor as key factors. Patients with no adverse outcomes were characterized primarily by high ADAMTS13, low syndecan-1, and low tissue factor. Interestingly, a subset of patients with high syndecan-1 but low tissue factor levels did not develop adverse outcomes, whereas those at high risk for adverse outcomes had low syndecan-1 but high tissue factor. It is thus implied that high tissue factor level may better predict death or MOF, though high syndecan-1 levels have a well-known correlation with EOT in previous (14, 43) and current studies. It is possible that these identified high-risk subpopulations are those that may benefit most from targeted therapeutics such as rADAMTS13.

Clinically, hemorrhagic shock patients are deemed “resuscitated” after achieving hemostasis, correcting coagulopathy, and restoring a normal acid-base status. However, the current study corroborates with other trauma studies showing sustained endothelial dysfunction for at least 24 hours. This phenomenon may be explained by reduced VWF cleavage at 24 hours compared to admission, which is associated with insufficient mobilization of ADAMTS13. Since much of the imbalance between VWF and ADAMTS13 was mediated by higher VWF, we investigated the potential benefit of supplementation with rhADAMTS13 in a mouse model of severe polytrauma and HS without blood product-based resuscitation (31,44). ADAMTS13 administration decreased total VWF-Ag and VWF:CB and improved VWF cleavage. These changes were accompanied by improved pulmonary histopathology and permeability. Our results support an

early report by Kleinveld et al. using a similar rat model (4). Together, our human and mouse studies delineate a causal role of VWF in accelerating endothelial injuries after severe trauma-HS and suggest a potentially novel therapeutic for treating EOT. However, excessive ADAMTS13 may increase the risk for bleeding (45, 46); therefore, any future clinical studies would need to perform careful dose-response and timing studies to achieve homeostatic balance between VWF and ADAMTS13.

Although an imbalance between VWF and ADAMTS13 in trauma-shock has been previously reported (4), our study is novel in: 1) developing an AI model to assess contributions of VWF-ADAMTS13 axis, along with common trauma markers to stratify outcomes of patients, 2) showing that A2 binding is a more precise to detect intrinsically active VWF using a high throughput method, 3) demonstrating a systemic oxidative stress state that persists for over 24 hours post-trauma, thereby defining a modification by which VWF becomes more active, 4) suggest an alternative pathway of how VWF adhesive activity is modified by oxidative stress and the role of ADAMTS13 in regulating the activity through proteolytic and potentially none-enzymatic means, (5) studied the imbalance of VWF-ADAMTS13 axis in patients and animal models. This approach allowed the cross-validation of data to identify measurements that are consistent between humans and mice and those that are not. This cross validation provides critical information for using animal models to study trauma pathophysiology and is impossible to achieve through a clinical or animal study alone.

Our study has several limitations. First, it has a limited sample size of HS patients that encompassed a range of transfusion requirements, such that important findings may have been masked. Second, we did not measure ADAMTS-13 activity using the conventional FRET-VWF-73 assay. This is intentional because this assay is designed to detect ADAMTS13 activity in

patients with TTP and is limited in quantifying the rate of VWF cleavage in individual patients. Therefore, we used a MS-based assay to directly measure VWF cleavage and calculated the ADAMTS13-to VWF-A2 ratio as markers for VWF hyperadhesive activity. We also do not know the ADAMTS13 concentrations in the transfused blood products. Lastly, our animal model only studied outcomes at a 3-hr timepoint, thus we cannot comment on the VWF cleavage rate immediately following trauma and hemorrhagic shock.

In conclusion, the present study supports a conclusion that VWF to ADAMTS13 imbalance drives, at least in part, the endothelial dysfunction and its associated adverse outcomes in traumatic HS patients. Using a novel MS-based proteomic approach, we demonstrated a significant reduction in VWF cleavage that was not improved by standard-of-care blood-product based resuscitation. Our findings support further investigation into rhADAMTS13 as a potential therapeutic and provide the premise for clinical studies to evaluate the efficacy of rhADAMTS13 therapy for severely injured patients with hemorrhagic shock.

Reference List

1. Eastridge BJ, Holcomb JB, Shackelford S. Outcomes of traumatic hemorrhagic shock and the epidemiology of preventable death from injury. Transfusion. 2019;59(S2):1423-1428.
2. Naumann DN, Hazeldine J, Davies DJ, et al. Endotheliopathy of trauma is an on-scene phenomenon, and is associated with multiple organ dysfunction syndrome: a prospective observational study. Shock. 2018;49(4):420-428.
3. Diebel LN, Liberati DM. Effect of tranexamic acid on endothelial von Willebrand factor/ADAMTS-13 response to in vitro shock conditions. J Trauma Acute Care Surg. 2023;94(2):273-280.
4. Kleinveld DJB, Simons DDG, Dekimpe C, et al. Plasma and rhADAMTS13 reduce trauma-induced organ failure by restoring the ADAMTS13-VWF axis. Blood Adv. 2021;5(17):3478-3491.
5. Wu Y, Liu W, Zhou Y, et al. von Willebrand factor enhances microvesicle-induced vascular leakage and coagulopathy in mice with traumatic brain injury. Blood. 2018;132(10):1075-1084.
6. Xu X, Wang C, Wu Y, et al. Conformation-dependent blockage of activated VWF improves outcomes of traumatic brain injury in mice. Blood. 2021;137(4):544-555.
7. Mayadas TN, Wagner DD. In vitro multimerization of von Willebrand factor is triggered by low pH. Importance of the propolypeptide and free sulfhydryls. J Biol Chem. 1989;264(23):13497-13503.
8. Vischer UM, Wagner DD. von Willebrand factor proteolytic processing and multimerization precede the formation of Weibel-Palade bodies. Blood. 1994;83(12):3536-3544.
9. Brouland JP, Egan T, Roussi J, et al. In vivo regulation of von willebrand factor synthesis: von Willebrand factor production in endothelial cells after lung transplantation between normal pigs and von Willebrand factor-deficient pigs. Arterioscler Thromb Vasc Biol. 1999;19(12):3055-3062.
10. Sporn LA, Marder VJ, Wagner DD. Inducible secretion of large, biologically potent von Willebrand factor multimers. Cell. 1986;46(2):185-190.
11. Counts RB, Paskell SL, Elgee SK. Disulfide bonds and the quaternary structure of factor VIII/von Willebrand factor. J Clin Invest. 1978;62(3):702-709.
12. Fowler WE, Fretto LJ, Hamilton KK, Erickson HP, McKee PA. Substructure of human von Willebrand factor. J Clin Invest. 1985;76(4):1491-1500.

13. Moake JL, Chow TW. Increased von Willebrand factor (vWf) binding to platelets associated with impaired vWf breakdown in thrombotic thrombocytopenic purpura. J Clin Apher. 1998;13(3):126-132.

14. Zeineddin A, Wu F, Chao W, et al. Biomarkers of endothelial cell dysfunction persist beyond resuscitation in patients with hemorrhagic shock. J Trauma Acute Care Surg. 2022;93(5):572-578.

15. Barry M, Pati S. Targeting repair of the vascular endothelium and glycocalyx after traumatic injury with plasma and platelet resuscitation. Matrix Biol Plus. 2022;14:100107.

16. Arya M, Anvari B, Romo GM, et al. Ultralarge multimers of von Willebrand factor form spontaneous high-strength bonds with the platelet glycoprotein Ib-IX complex: studies using optical tweezers. Blood. 2002;99(11):3971-3977.

17. Furlan M, Robles R, Lämmle B. Partial purification and characterization of a protease from human plasma cleaving von Willebrand factor to fragments produced by in vivo proteolysis. Blood. 1996;87(10):4223-4234.

18. Chauhan AK, Goerge T, Schneider SW, Wagner DD. Formation of platelet strings and microthrombi in the presence of ADAMTS-13 inhibitor does not require P-selectin or beta3 integrin. J Thromb Haemost. 2007;5(3):583-589.

19. Dong JF, Moake JL, Nolasco L, et al. ADAMTS-13 rapidly cleaves newly secreted ultralarge von Willebrand factor multimers on the endothelial surface under flowing conditions. Blood. 2002;100(12):4033-4039.

20. Padilla A, Moake JL, Bernardo A, et al. P-selectin anchors newly released ultralarge von Willebrand factor multimers to the endothelial cell surface. Blood. 2004;103(6):2150-2156.

21. Levy GG, Nichols WC, Lian EC, et al. Mutations in a member of the ADAMTS gene family cause thrombotic thrombocytopenic purpura. Nature. 2001;413(6855):488-494.

22. Tsai HM. Physiologic cleavage of von Willebrand factor by a plasma protease is dependent on its conformation and requires calcium ion. Blood. 1996;87(10):4235-4244.

23. Tsai HM, Sussman II, Nagel RL. Shear stress enhances the proteolysis of von Willebrand factor in normal plasma. Blood. 1994;83(8):2171-2179.

24. Holcomb JB, Tilley BC, Baraniuk S, et al. Transfusion of plasma, platelets, and red blood cells in a 1:1:1 vs a 1:1:2 ratio and mortality in patients with severe trauma: the PROPPR randomized clinical trial. JAMA. 2015;313(5):471-482.

25. Vasquez M, Abdullah S, Rehani C, et al. Ongoing endothelial cell dysfunction following hemorrhagic shock: crystalloids are the culprit. Shock. 2026;66(1):51-57.

26. Sauaia A, Moore EE, Johnson JL, et al. Temporal trends of postinjury multiple-organ failure: still resource intensive, morbid, and lethal. J Trauma Acute Care Surg. 2014;76(3):582-592.

27. Liu W, Patel K, Wang Y, et al. Dynamic and functional linkage between von Willebrand factor and ADAMTS-13 with aging: an atherosclerosis risk in community study. J Thromb Haemost. 2023;21(12):3371-3382.

28. Yang M, Houck KL, Dong X, et al. Hyperadhesive von Willebrand factor promotes extracellular vesicle-induced angiogenesis: implication for LVAD-induced bleeding. JACC Basic Transl Sci. 2022;7(3):247-261.

29. Chen J, Fu X, Wang Y, et al. Oxidative modification of von Willebrand factor by neutrophil oxidants inhibits its cleavage by ADAMTS13. Blood. 2010;115(3):706-712.

30. MacArthur TA, Goswami J, Navarro SM, et al. A murine multiple-injury model for the study of thromboinflammation. J Trauma Acute Care Surg. 2024;96(2):203-208.

31. Zeineddin A, Wu F, Dong JF, et al. Early lyophilized cryoprecipitate enhances the ADAMTS13/VWF ratio to reduce systemic endotheliopathy and lessen lung injury in a mouse multiple-trauma hemorrhage model. J Trauma Acute Care Surg. 2023;95(2S Suppl 1):S137-S143.

32. Hastie T, Tibshirani R, Friedman J. The Elements of Statistical Learning: Data Mining, Inference, and Prediction. 2nd ed. Springer Series in Statistics; 2009.

33. Fu X, Cate SA, Dominguez M, et al. Cysteine disulfides (Cys-ss-X) as sensitive plasma biomarkers of oxidative stress. Sci Rep. 2019;9(1):115.

34. Gao D, Zhou Z, Ma R, et al. Recombinant ADAMTS-13 improves survival of mice subjected to endotoxemia. Int J Mol Sci. 2023;24(14):11782.

35. Hatton GE, Isbell KD, Henriksen HH, et al. Endothelial dysfunction is associated with increased incidence, worsened severity, and prolonged duration of acute kidney injury after severe trauma. Shock. 2021;55(3):311-315.

36. Dyer MR, Plautz WE, Ragni MV, et al. Traumatic injury results in prolonged circulation of ultralarge von Willebrand factor and a reduction in ADAMTS13 activity. Transfusion. 2020;60(6):1308-1318.

37. Russell RT, McDaniel JK, Cao W, et al. Low plasma ADAMTS13 activity is associated with coagulopathy, endothelial cell damage and mortality after severe paediatric trauma. Thromb Haemost. 2018;118(4):676-687.

38. Siemiatkowski A, Kłoczko J, Wereszczyńska-Siemiatkowska U, et al. Effect of severe multiple trauma complicated by acute lung injury on endothelial cell activity. Przegl Lek. 2001;58(7-8):767-771.

39. Plautz WE, Haldeman SH, Dyer MR, et al. Reduced cleavage of von willebrand factor by ADAMTS13 is associated with microangiopathic acute kidney injury following trauma. Blood Coagul Fibrinolysis. 2022;33(1):14-24.

40. Zeineddin A, Dong JF, Wu F, Terse P, Kozar RA. Role of von Willebrand factor after injury: it may do more than we think. Shock. 2021;55(6):717-722.

41. Martin C, Morales LD, Cruz MA. Purified A2 domain of von Willebrand factor binds to the active conformation of von Willebrand factor and blocks the interaction with platelet glycoprotein Ibalpha. J Thromb Haemost. 2007;5(7):1363-1370.

42. Butera D, Passam F, Ju L, et al. Autoregulation of von Willebrand factor function by a disulfide bond switch. Sci Adv. 2018;4(2):eaaq1477.

43. Rodriguez EG, Ostrowski SR, Cardenas JC, et al. Syndecan-1: a quantitative marker for the endotheliopathy of trauma. J Am Coll Surg. 2017;225(3):419-427.

44. Scully M, Antun A, Cataland SR, et al. Recombinant ADAMTS13 in congenital thrombotic thrombocytopenic purpura. N Engl J Med. 2024;390(17):1584-1596.

45. Roberts TR, Villalobos PA, Bigon EB, et al. von Willebrand factor dynamics in trauma managed with extracorporeal life support. J Thromb Haemost. 2026;24(5)1677-1689.

46. Stockschlaeder M, Schneppenheim R, Budde U. Update on von Willebrand factor multimers: focus on high-molecular-weight multimers and their role in hemostasis. Blood Coagul Fibrinolysis. 2014;25(3):206-216.

TABLES

Table 1. Hemorrhagic Shock (HS) Cohort and Subcohort

Parameter	HS Cohort n=100	HS Subcohort n=10	p value
Age years median IQR	39 (31,53)	35 (32,53)	0.7
Male n(%)	81%	80%	0.9
Blunt mechanism n(%)	61%	70%	0.59
Systolic BP mm Mg median (IQR)	80 (70,85)	89(72,115)	0.6
Lactate mmol/L median IQR	6 (5,9)	7(6,10)	0.35

Table 2. Correlations between VWF and ADAMTS13 with indices of endotheliopathy and coagulopathy in high transfusion cohort

Correlations	Rho	p value	95% CI
VWF			
Syndecan	0.545	< 0.001	0.29 – 0.73
Platelets	0.353	0.016	0.07 – 0.52
Lactate	0.321	0.038	0.01 – 0.58
SOFA day 1	0.371	0.001	0.09 – 0.60
ADAMTS13			
Syndecan	0.578	< 0.001	0.34 – 0.75
Platelets	0.315	0.033	0.02 – 0.56
INR	0.337	0.022	0.04 – 0.58
PT	0.354	0.016	0.06 – 0.59
PTT	0.411	0.005	0.13 – 0.63
ISS	0.317	0.032	0.02 – 0.56
SOFA day 1	0.463	0.001	0.20 – 0.66
SOFA day 4	0.323	0.029	0.04 – 0.56
Ventilator days	0.360	0.014	0.08 – 0.59

ISS= injury severity score; SOFA- sequential organ failure assessment

Table 3. Variable Importance Measures (VIM) ranking factors from CART analysis.

Rank	Factor	VIM
1	Tissue Factor	100
2	Syndecan-1	65
3	Angiopoietin-2	46
4	PTT	41
5	Thrombomodulin	39
6	INR	39
7	ADAMTS13	35
8	PT	34
9	VWF:A2	21
10	P Selectin	14

CART= Classification and Regression Tree

Figure Legends

Figure 1. Markers of the endotheliopathy of trauma are increased in traumatic hemorrhagic shock patients compared to minimally injured patients. (A) IL-6, (B) syndecan-1, (C) angiopoietin-1, (D) Angiopoietin-2, (E) tissue factor, (F) thrombomodulin. ** $p<0.001$; data analyzed by Kruskal Wallis test. MI=minimally injured patients, blood drawn at admission; HS= hemorrhagic shock patients with blood drawn at the time of **ad**mission; n=100 HS and n=39 MI.

Figure 2. Correlation between VWF-A2 and ADAMTS13 and syndecan-1 and between VWF-A2 and ADAMTS13 in traumatic hemorrhagic shock patients. Plasma levels of VWF-A2 (A) and ADAMTS13 (B), and their ratio (C) between samples collected in hemorrhagic shock patients (HS) at admission versus minimally injured control samples collected at admission (MI); n=100; ** $p<0.001$. Scatterplots in patients receiving at least 8 units of blood products demonstrate the correlation between (D) VWF-A2 and syndecan-1 rho 0.545, $p<0.001$ and (E) ADAMTS13 and syndecan-1 rho 0.317, $p=0.032$ and (F) VWF-A2 and ADAMTS13 rho 0.502, $p<00001$. Data were analyzed by Spearman rho rank correlation, n=46

Figure 3. Classification and Regression Tree (CART) modeling. CART was used to identify multilevel interaction factors and extreme groups of patients with adverse outcomes (death or multiple organ failure). CART discovered patient groups with very high adverse effects (46.7% and 70.8%) and very low adverse effects (0%). Adverse outcomes defined as either death or a multiple organ failure score ≥ 3. ADAMTS13=A disintegrin and Metalloprotease with Thrombospondin motif-13, Ang-2=angiopoietin-2, , HS: hemorrhagic shock, TF=tissue factor; n=100.

Figure 4. Longitudinal changes in VWF, ADAMTS13, VWF cleavage level and protein-ss-Cys in traumatic hemorrhagic shock patients. (A) ratio of ADAMTS13 to VWF-A2, (B) VWF collagen binding, (C) VWF collagen binding activity, (D) Plasma levels of platelet-derived extracellular vesicles (EVs) that are VWF-bound ($VWF^+/CD41^+$ pEVs**).** Mass spectrometry was used to measure the (E) VWF cleavage and the (F) the percentage of protein-ss-Cys over time. * $p<0.05$, ** $p<0.001$; data analyzed using Kruskal-Wallis one way analysis of variance on ranks. MI=minimally injured patients, blood drawn at admission; AD= hemorrhagic shock patients with blood drawn at the time of **ad**mission; post= post resuscitation and 24 h=24 hours after admission; CB=collagen binding; n=10 HS and n=10MI.

Figure 5. Lung dysfunction, plasma levels of VWF and rates of VWF cleavage are improved after treatment with recombinant ADAMTS13 in mice subjected to polytrauma and hemorrhagic shock. C57BL/6 mice 9–10 weeks of age underwent polytrauma with bowel evisceration, tibia fracture and a muscle crush injury then hemorrhagic shock for 90 minutes (n=10). Mice were resuscitated with 1x lost blood volume lactated Ringers (LR) +/- the addition of recombinant ADAMTS13. Three hours later lungs and blood were harvested for (A) lung histopathologic injury, (B) bronchial alveolar lavage (BAL) protein as an indicator of lung permeability, (C) thrombi counts, (D) VWF collagen binding activity, (E) VWF:CB to VWF-Ag ratio, (F) VWF+ platelet EVs (CD41+) among all platelet EVs, and (G) VWF cleavage rate measured by mass spectrometry. Data was analyzed by one-way ANOVA corrected by Tukey multiple comparisons test; ** $p<0.001$.

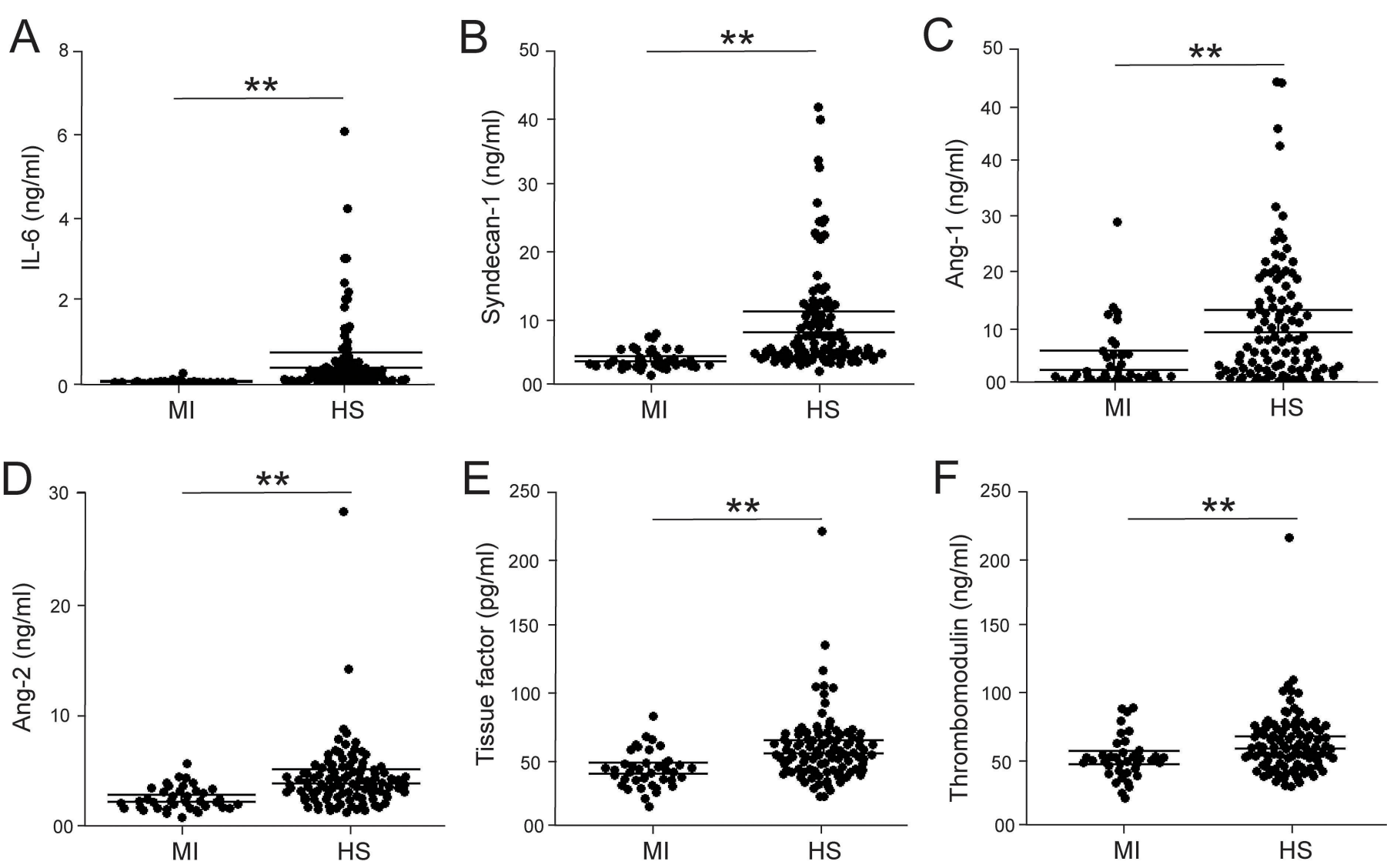
A
IL-6 (ng/ml)
8
6
4
2
0
**
MI
HS
B
Syndecan-1 (ng/ml)
50
40
30
20
10
00
**
MI
HS
C
Ang-1 (ng/ml)
50
40
40
30
20
10
00
**
MI
HS
D
Ang-2 (ng/ml)
30
20
10
00
**
MI
HS
E
Tissue factor (pg/ml)
250
200
150
100
50
00
**
MI
HS
F
Thrombomodulin (ng/ml)
250
200
150
100
50
00
**
MI
HS

A

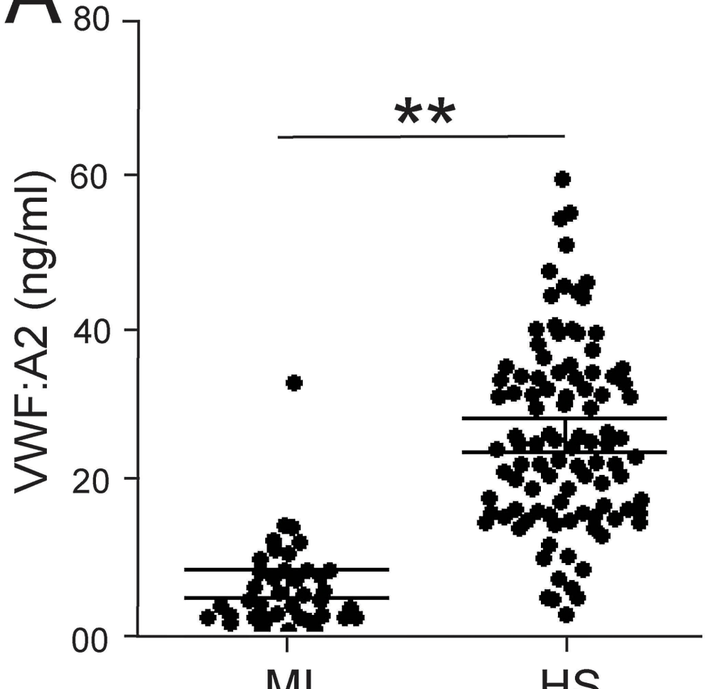
80
60
40
20
00
VWF:A2 (ng/ml)
**
MI
HS

B

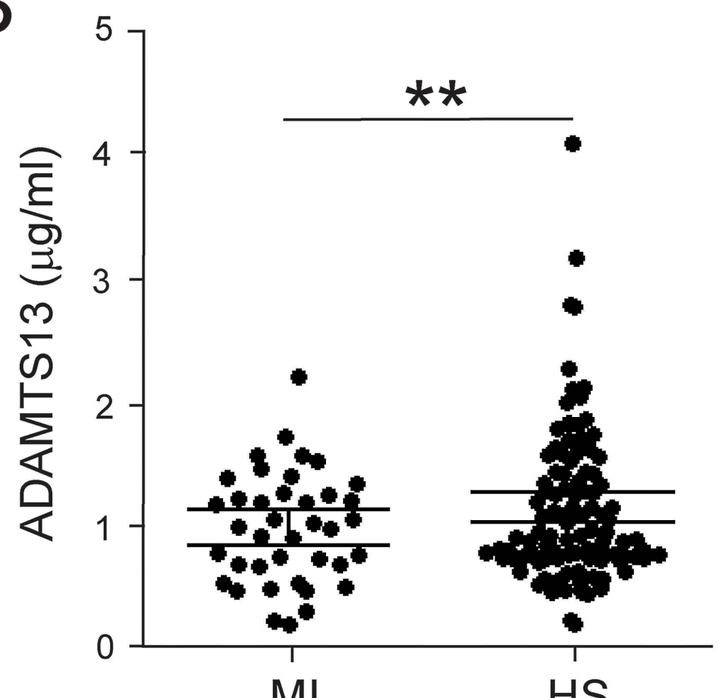
5
4
3
2
1
0
ADAMTS13 (μg/ml)
**
MI
HS

C

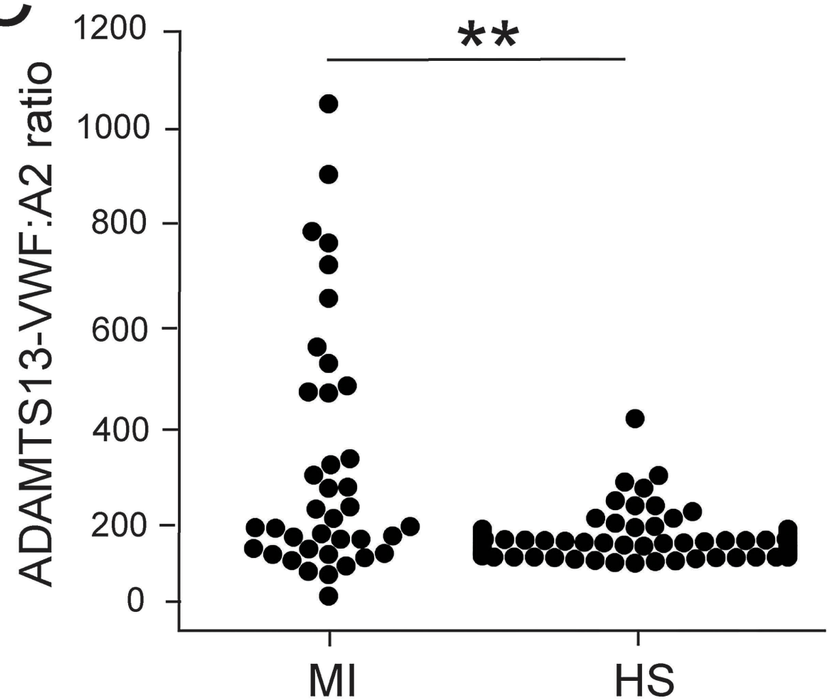
1200
1000
800
600
400
200
0
ADAMTS13-VWF:A2 ratio
**
MI
HS

D

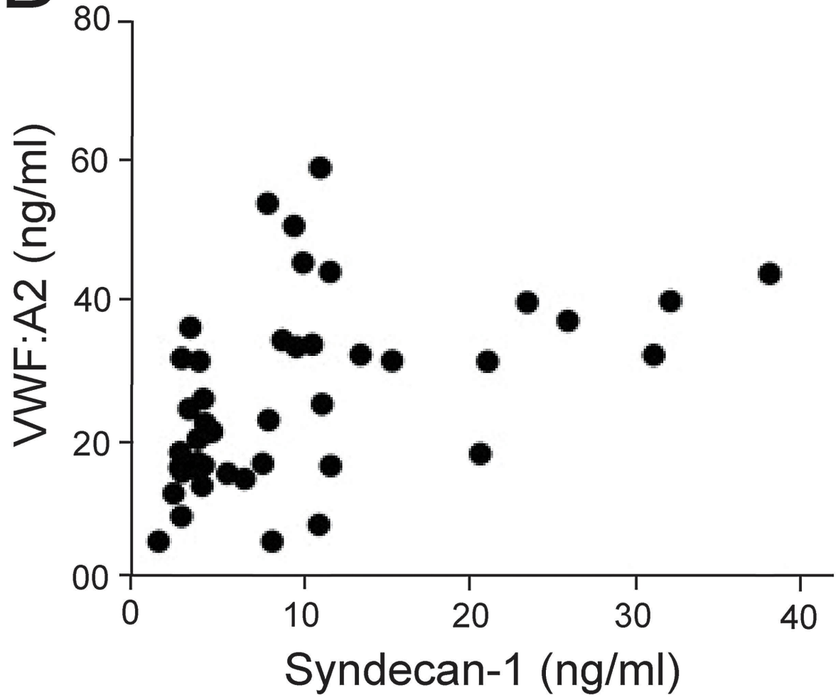
80
60
40
20
00
VWF:A2 (ng/ml)
0
10
20
30
40
Syndecan-1 (ng/ml)

E

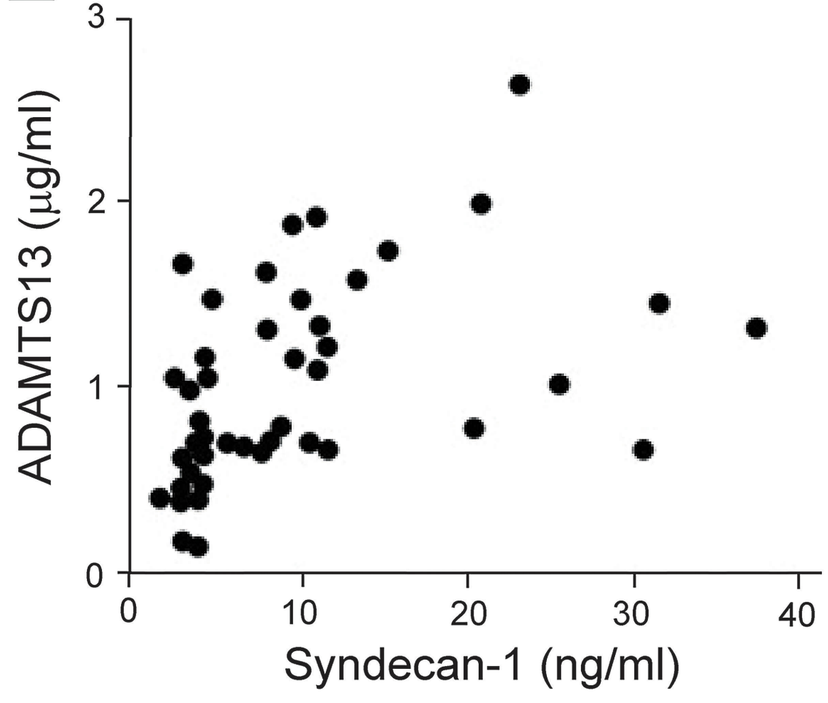
3
2
1
0
ADAMTS13 (μg/ml)
0
10
20
30
40
Syndecan-1 (ng/ml)

F

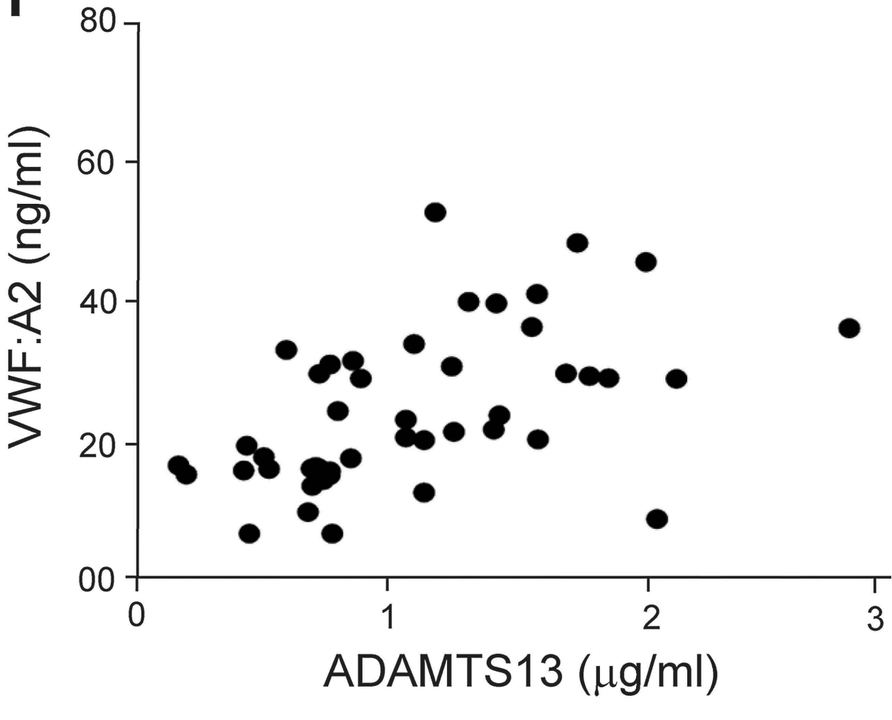
80
60
40
20
00
VWF:A2 (ng/ml)
0
1
2
3
ADAMTS13 (μg/ml)

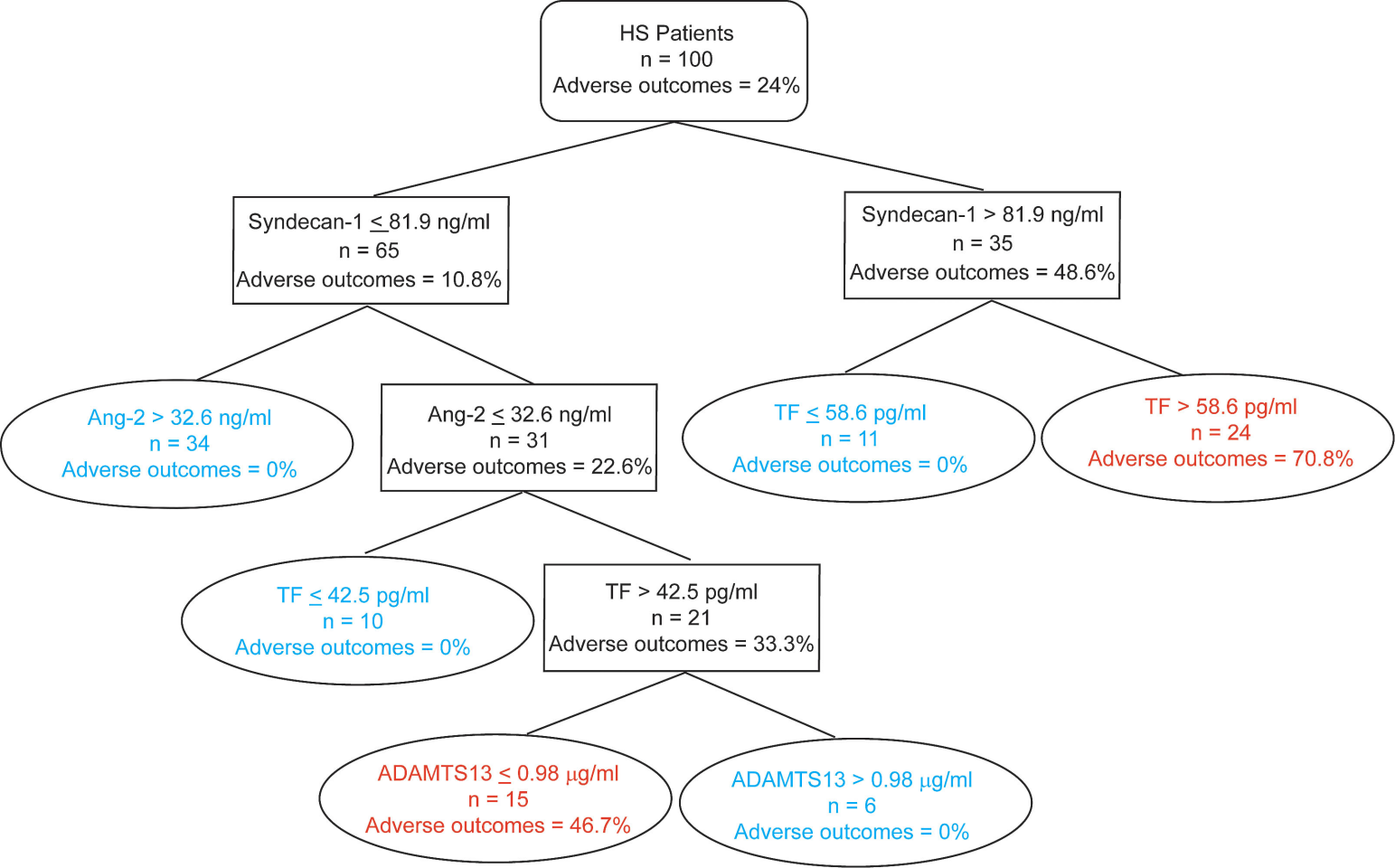
HS Patients
n = 100
Adverse outcomes = 24%
Syndecan-1 ≤ 81.9 ng/ml
n = 65
Adverse outcomes = 10.8%
Syndecan-1 > 81.9 ng/ml
n = 35
Adverse outcomes = 48.6%
Ang-2 > 32.6 ng/ml
n = 34
Adverse outcomes = 0%
Ang-2 ≤ 32.6 ng/ml
n = 31
Adverse outcomes = 22.6%
TF ≤ 58.6 pg/ml
n = 11
Adverse outcomes = 0%
TF > 58.6 pg/ml
n = 24
Adverse outcomes = 70.8%
TF ≤ 42.5 pg/ml
n = 10
Adverse outcomes = 0%
TF > 42.5 pg/ml
n = 21
Adverse outcomes = 33.3%
ADAMTS13 ≤ 0.98 μg/ml
n = 15
Adverse outcomes = 46.7%
ADAMTS13 > 0.98 μg/ml
n = 6
Adverse outcomes = 0%

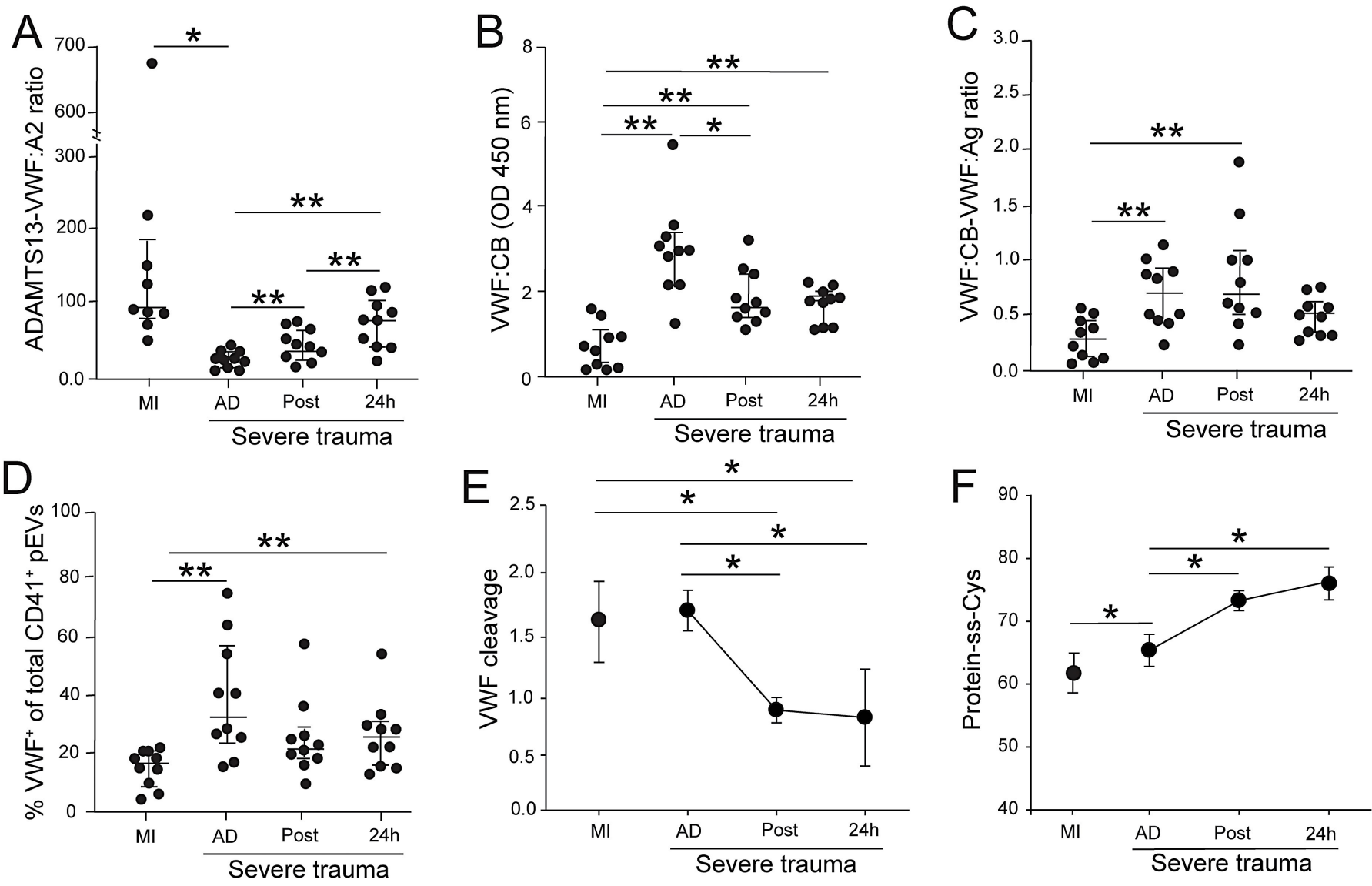
A
ADAMTS13-VWF:A2 ratio
700
600
300
200
100
0.0
MI
AD
Post
24h
Severe trauma
B
VWF:CB (OD 450 nm)
8
6
4
2
0
C
VWF:CB-VWF:Ag ratio
3.0
2.5
2.0
1.5
1.0
0.5
0.0
D
% VWF+ of total CD41+ pEVs
100
80
60
40
20
0
E
VWF cleavage
2.5
2.0
1.5
1.0
0.5
0.0
F
Protein-ss-Cys
90
80
70
60
50
40

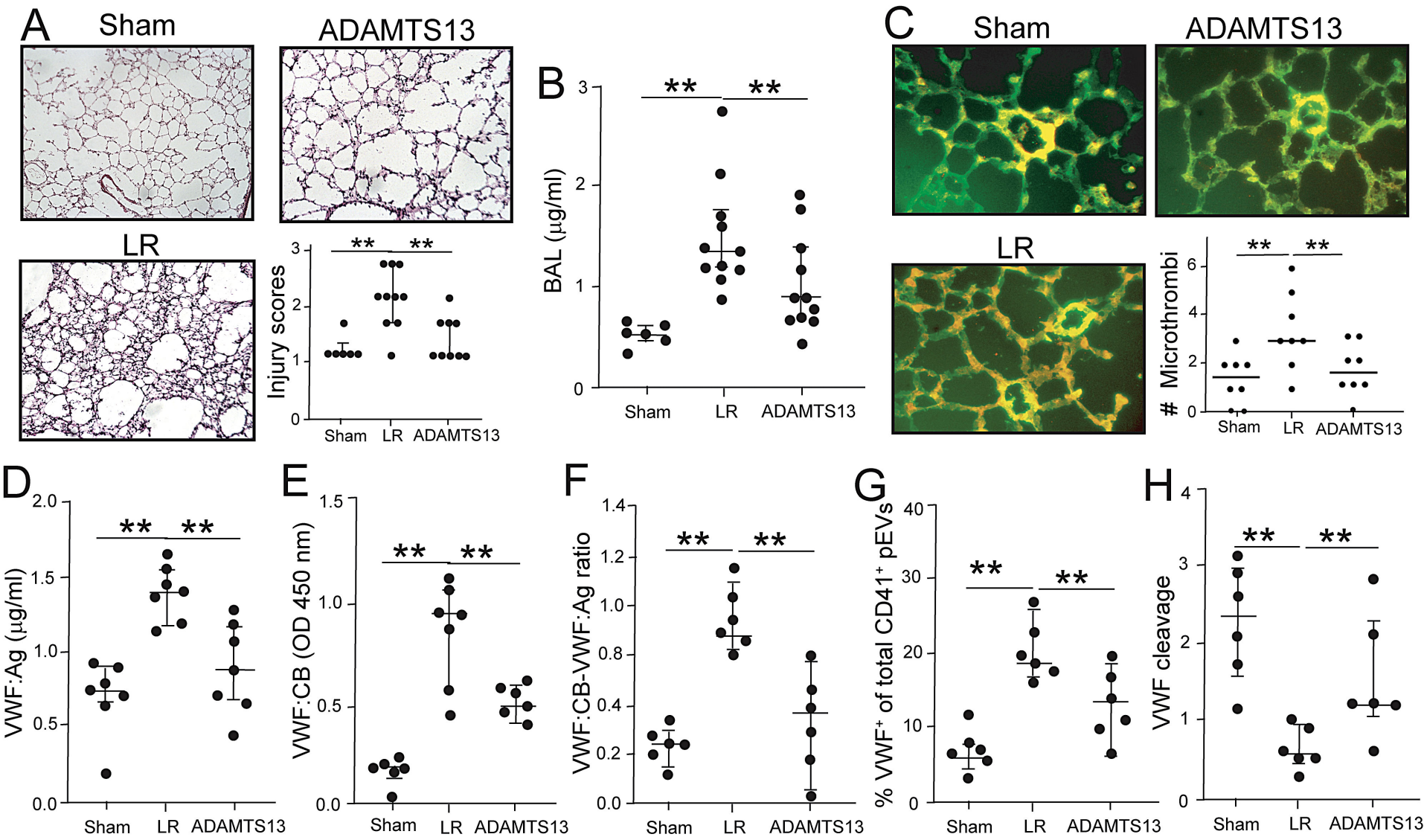
A
Sham
ADAMTS13
LR
Injury scores
Sham
LR
ADAMTS13
B
BAL (μg/ml)
Sham
LR
ADAMTS13
C
Sham
ADAMTS13
LR
Microthrombi
Sham
LR
ADAMTS13
D
VWF:Ag (μg/ml)
Sham
LR
ADAMTS13
E
VWF:CB (OD 450 nm)
Sham
LR
ADAMTS13
F
VWF:CB-VWF:Ag ratio
Sham
LR
ADAMTS13
G
% VWF+ of total CD41+ pEVs
Sham
LR
ADAMTS13
H
VWF cleavage
Sham
LR
ADAMTS13

SUPPLEMENTAL MATERIALS AND METHODS

Human study: Inclusion criteria were patients who were transferred from the scene within 2 hours of injury, had blood pressure (BP)<90 mm Hg attributable to blood loss and receiving at least one unit of whole blood or ≥2 units of any blood component (**Supplemental Figure 1**). Exclusion criteria included cardiopulmonary arrest prior to arrival, > 2 hours from injury, traumatic brain injury (head AIS ≥3), pregnancy, prisoner, on anticoagulant medication. Waiver of consent was granted when admission blood samples were collected from waste blood. Consent was obtained from all patients or their legally authorized representative when samples were collected at post resuscitation and at 24 hours. Samples were collected in EDTA tubes, plasma isolated then stored at -80C° until use. Minimally injured (MI) patients were used as control and they were defined as an injury severity score (ISS) <9.

Classification and Regression Tree (CART): The CART model is a statistical method that divides the sample into subgroups of patients with similar risks of an adverse outcome, producing highly distinctive risk groups, typically low- and high-risk groups, with the possibility of an intermediate risk group as well. The splitting criterion is group homogeneity measured by the Gini index. The variable that yields the greatest improvement in the Gini index is selected. CART models are nonparametric recursive partitioning models that are not affected by extreme values and can work with missing data without imputations and without excluding any observations. To avoid overfitting the data, CART model is estimated on the full sample using 10-fold cross-validation: ten separate models are fit, each trained on 9/10 of the sample, with the remaining tenth used for validation. The results of the ten models are then averaged, and the averaged results are reported as the final estimates. Quality ascertained by Area Under the

Receiver Operating Curve (AUROC) for the validation data that were not used to build the model.

VWF-A2: Plasma VWF-A2 was detected using Luminex by an antibody made specifically against the VWF-A2 domain because VWF A1 and A2 domains form a complex (1) during homeostasis to make VWF inactive. This A1-A2 complex is disrupted when the two vicinal cysteine residues in A2 domain are oxidized (2), potentially in the oxidative stress environment of trauma to expose the A2 domain for detection. This confirmation change activates VWF to bind platelets but does not increase VWF cleavage because selective methionine oxidation of VWF (3).

VWF antigen (VWF-Ag) and collagen binding (VWF:CB): VWF-Ag was measured by two ELISA kits for human and mouse VWF, respectively (kit#ab168548 and ab208980, Abcam, Waltham, MA) (4, 5). VWF:CB was measured using an ELISA kit (kit#5450311, DiaPharma, West Chester, OH). This assay is widely used to measure VWF adhesive activity and also used for estimating the VWF-cleaving activity of ADAMTS13 (6).

ADAMTS13 cleavage of VWF in humans and mice: ADAMTS13 activity is often measured by detecting cleaved VWF multimers using immunoblots (7) or quantifying the cleavage rate of a recombinant VWF-A2 peptide of 73 amino acids in an assay called FRET-VWF-73 (8). However, the former is only semi-quantitative, whereas the latter cannot define VWF cleavage in individual patients, which varies considerably and is affected by non-ADAMTS13 factors. For example, VWF from trauma patients could be resistant to cleavage by ADAMTS13 because of VWF oxidation (3). To overcome these limitations, we developed a nano flow liquid chromatography tandem mass spectrometry (nano LC-MS/MS) assay. This assay detected the tryptic peptide EQAPNLVY, which is formed only when VWF is cleaved by ADAMTS13

(uncleaved tryptic peptide is EQAPNLV$\underline{Y^{1605}M^{1606}}$VTGNPASDEIK, the Y^{1605}-M^{1606} peptide bond is underlined). We also detected the reference peptide EAPDLVLQR and calculated the EQAPNLVY-to-EAPDLVLQR ratio as the rate of VWF cleavage. As a control, we quantified the rate of VWF cleavage in plasma pooled from healthy subjects.

Methodology for nano flow liquid chromatography tandem mass spectrometry

For human studies, VWF was immunoprecipitated from 0.05 ml of plasma samples from patients and controls using a polyclonal rabbit anti-human VWF antibody (#A0082, Dako, Santa Clara, CA) coupled to magnetic protein G DynaBeads (Invitrogen, Waltham, MA). The immunoprecipitated VWF was eluted from the beads, reduced by dithiothreitol, alkylated by iodoacetamide, and digested by trypsin. To quantify VWF cleavage, the tryptic peptides were mixed with known amounts of two heavy isotope-labelled peptides, EQAPNL*VY and EAPDL*VLQR (L*: U-13C6 15N L, Anaspec, Fremont, CA). VWF tryptic peptides were detected using nano flow liquid chromatography tandem mass spectrometry (nano LC-MS/MS) on a ThermoFisher Scientific Orbitrap Fusion™ Lumos™ Tribrid mass spectrometer coupled with a ThermoFisher Scientific UltiMate™ 3000 RSLCnano system. Peptides were separated at a flow rate of 300 nL/min on an Acclaim™ PepMap™ 100 C18 column (0.075 x 250mm, 2 μm, ThermoFisher Scientific), using solvent A (0.1% formic acid and 2% acetonitrile in water) and solvent B (0.1% formic acid in acetonitrile). They were eluted through a linear gradient of 2%-18% solvent B over 100 min.

To further investigate the effect of rhADAMTS13 on reducing trauma/HS-induced lung injury, we modified the MS method to quantify mouse VWF cleavage rate because the sequence of tryptic peptide of mouse VWF cleaved by ADAMTS13 differs from that of human VWF (**Supplemental Figure 2**). We validated the mouse methodology by measuring the increase of

cleaved tryptic peptide VEAPNLVY and the decrease of the uncleaved VEAPNLVYMVTGNPASDEIK peptide of recombinant mouse VWF in an incubation time dependent manner (**Supplemental Figure 6**). Mouse VWF was again immunoprecipitated from plasma samples using a protocol identical to that of human VWF. The immunoprecipitated VWF was again reduced with dithiothreitol, alkylated with iodoacetamide, and digested with trypsin/Lys-C (Promega, Madison, WI). The resultant tryptic VWF peptides were spiked with two heavy isotope-labeled peptides: VEAPNL*VY, which was the tryptic VWF-A2 peptide cleaved by ADAMTS13 (the tryptic peptide uncleaved by ADAMTS13 is VEAPNLVYMVTGNPASDEIK; the cleavage site is underlined) and DFETL*PR, which is a control tryptic peptide from the VWF-A2 domain downstream from the cleavage site (L*: U-$^{13}C_6$ ^{15}N L, Genscript). Tryptic mouse VWF peptides were analyzed by nano-LC-MS/MS using a Thermo Scientific Orbitrap Fusion™ Lumos™ Tribrid mass spectrometer coupled to a Vanquish Neo UHPLC system. Separation was performed at a 400 nL/min flow rate on an Ionopticks Aurora Ultimate XT column (25 cm × 75 µm, C18). The cleavage of the Y^{1605}-M^{1606} bond by ADAMTS13 was quantified by calculating the ratio of cleaved peptide VEAPNLVY to the control peptide DFETLPR.

To minimize potential sample preparation–related methionine oxidation, 5 mM methionine (Met) was included in all sample preparation processes, including VWF immunoprecipitation, trypsin digestion, and sample suspension solution. The excess amount of free Met prevents protein oxidation during sample processing because oxidizing free methionine residues is favored in kinetic over those in proteins (9).

Methionine oxidation was determined by dividing the peak area of oxidized peptides by the total peak area of oxidized and unoxidized forms. The degree of VWF methionine oxidation was

reported as the number of patients whose ratios of oxidized-to-total Met1303, Met1304, Met1385, Met1606, Met1521, Met1761, and Met1860 were greater than 1 per VWF monomer (i.e., enhanced methionine oxidation). Protein-ss-Cys, which was the total amount of plasma proteins that formed mix-disulfide-bound with the plasma glutathione, was quantified using LC-MS/MS, as we previously reported (10). Levels of plasma protein-ss-Cys served as the surrogate marker for the overall oxidative stress in plasma samples. Oxidative stress can induce: 1) methionine oxidation of VWF, which could change the rate of VWF cleavage by ADAMTS13, 2) conformational changes of VWF, rendering VWF hyperadhesive, and 3) the lateral association to form VWF fibrils (11). Levels of protein-ss-Cys were calculated as the difference between total small molecule Cys and Cys-containing disulfides, divided by total Cys.

Flow cytometry in humans and mice

Flow cytometry was used to detect levels of VWF-bound platelet-derived extracellular vesicles (EV) in plasma samples from trauma patients and mice as we previously described (5). Briefly, samples were incubated with an FITC-conjugated antibody against the platelet marker CD41a (EPR4330, Abcam, Waltham, MA), and an APC-anti-VWF antibody (F8/88, ThermoFisher Scientific, Waltham, MA). Samples were analyzed in the EV gate set using standard microbeads (A34305, ThermoFisher Scientific, Waltham, MA) to specifically detect VWF-bound platelet EVs.

Mice model and assays

Research was conducted in accordance with an approved animal use protocol at an AAALAC International-accredited facility, in full compliance with all applicable federal statutes and regulations governing the use of animals in research. The study adhered to the principles outlined

in the Guide for the Care and Use of Laboratory Animals (National Research Council, 2011 edition). The Animal Care and Use Committee of Institutes of the University of Maryland School of Medicine approved the animal use protocol (IACUC #0422005).

C57BL/6 (9–10 weeks of age, Jackson Laboratories, Bar Harbor, ME) male and female mice in an 8:2 ratio (reflected human trauma cohort) underwent isoflurane anesthesia. Mice were provided with water and food *ad libitum* and allowed to acclimate to the housing for at least 7 days. The femoral artery and vein cannulated for hemodynamic monitoring and blood withdrawal /resuscitation. The polytrauma model included laparotomy, unilateral tibia fracture and a gastrocnemius muscle crush followed by hemorrhagic shock induction (mean arterial pressure (MAP) of 35 ± 5 mm Hg for 90 minutes. Hypotensive resuscitation entailed infusion of lactated Ringer's to a MAP 55-60 mmHg for 3 hours to simulate prehospital transport and time to hemorrhage control. Shams underwent anesthesia and catheter placement without trauma or shock. No animals were excluded. Mice were assigned to different experimental groups by randomly allocating them to each group. Sample size was based on our previous studies using a mouse model of multiple-trauma and hemorrhage shock and a mouse model using recombinant ADAMTS13 (12, 13).

After completion of 3 hr resuscitation, mouse bronchoalveolar lavage was collected and stored at -80ºC until analysis. Total protein in bronchoalveolar lavage was measured with the BCA protein assay (kit#23228, ThermoFisher Scientific, Rockford, IL) as an indicator of lung permeability. Lung tissues were snap-frozen in OCT and sectioned by a cryostat (CM3050, Leica, Deer Park, IL). The sections were stained with hematoxylin and eosin (H&E) and observed under a fluorescent microscope (FM820T-18M3, AmScope, Irvine, CA). The images were taken by an CCD camera (Infinity 2, Lumenera, Ottawa, Canada) and scored for alveolar thickness, capillary

congestion, and leukocyte infiltration (14, 15) as an indicator of lung inflammation. Lung tissue was also co-stained with a VWF polyclonal antibody (#27186-1-AP, ThermoFisher Scientific, Waltham, MA) and an anti-fibrin mouse monoclonal antibody (#MABS2155, MilliporeSigma, Burlington, MA) as a marker of microvascular thrombi as we have described (16). Blood was harvested via cardiopuncture and centrifuged at 2,000xg for 10 min at room temperature. Plasma was collected and stored at -80°C until analysis.

References

1. Martin C, Morales LD, Cruz MA. Purified A2 domain of von Willebrand factor binds to the active conformation of von Willebrand factor and blocks the interaction with platelet glycoprotein Ibalpha. J Thromb Haemost. 2007;5(7):1363-1370.
2. Butera D, Passam F, Ju L, et al. Autoregulation of von Willebrand factor function by a disulfide bond switch. Sci Adv. 2018;4(2):eaaq1477.
3. Chen J, Fu X, Wang Y, et al. Oxidative modification of von Willebrand factor by neutrophil oxidants inhibits its cleavage by ADAMTS13. Blood. 2010;115(3):706-712.
4. Xu X, Wang C, Wu Y, et al. Conformation-dependent blockage of activated VWF improves outcomes of traumatic brain injury in mice. Blood. 2021;137(4):544-555.
5. Yang M, Houck KL, Dong X, et al. Hyperadhesive von Willebrand Factor Promotes Extracellular Vesicle-Induced Angiogenesis: Implication for LVAD-Induced Bleeding. JACC Basic Transl Sci. 2022;7(3):247-261.
6. Gerritsen HE, Turecek PL, Schwarz HP, et al. Assay of von Willebrand factor (vWF)-cleaving protease based on decreased collagen binding affinity of degraded vWF: a tool for the diagnosis of thrombotic thrombocytopenic purpura (TTP). Thromb Haemost. 1999;82(5):1386-1389.
7. Tsai HM, Sussman II, Nagel RL. Shear stress enhances the proteolysis of von Willebrand factor in normal plasma. Blood. 1994;83(8):2171-2179.
8. Kokame K, Nobe Y, Kokubo Y, Okayama A, Miyata T. FRETS-VWF73, a first fluorogenic substrate for ADAMTS13 assay. Br J Haematol. 2005;129(1):93-100.
9. Liu W, Patel K, Wang Y, et al. Dynamic and functional linkage between von Willebrand factor and ADAMTS-13 with aging: an Atherosclerosis Risk in Community study. J Thromb Haemost. 2023;21(12):3371-3382.
10. Fu X, Cate SA, Dominguez M, et al. Cysteine Disulfides (Cys-ss-X) as Sensitive Plasma Biomarkers of Oxidative Stress. Sci Rep. 2019;9(1):115.

11. Choi H, Aboulfatova K, Pownall HJ, Cook R, Dong JF. Shear-induced disulfide bond formation regulates adhesion activity of von Willebrand factor. J Biol Chem. 2007;282(49):35604-35611.
12. Zeineddin A, Wu F, Dong JF, et al. Early lyophilized cryoprecipitate enhances the ADAMTS13/VWF ratio to reduce systemic endotheliopathy and lessen lung injury in a mouse multiple-trauma hemorrhage model. J Trauma Acute Care Surg. 2023;95(2S Suppl 1): S137-S143.
13. Wu Y, Liu W, Zhou Y, et al. von Willebrand factor enhances microvesicle-induced vascular leakage and coagulopathy in mice with traumatic brain injury. Blood. 2018; 132(10):1075-1084.
14. Hart ML, Ceonzo KA, Shaffer LA, et al. Gastrointestinal ischemia-reperfusion injury is lectin complement pathway dependent without involving C1q. J Immunol. 2005;174(10):6373-6380.
15. Wu F, Dorman B, Zeineddin A, Kozar RA. Fibrinogen inhibits metalloproteinase-9 activation and syndecan-1 cleavage to protect lung function in apoe null mice after hemorrhagic shock. J Surg Res. 2023;288:208-214.
16. Zeineddin A, Wu F, Dong JF, et al. Trauma-derived extracellular vesicles are sufficient to induce endothelial dysfunction and coagulopathy. Shock. 2022;58(1):38-44.

Table S1. Methionine Oxidation of VWF in hemorrhagic shock patients*

Methionine	Minimally injured (n=10)	Patients with severe trauma (n=10)			p value#
	% total	Admission	Post resuscitation	24 hours post admission	
Met1303	6.5	20	40	50	p <0.05
Met1304	8.2	20	10	20	NS
Met1385	5.2	71	30	38	p <0.05
Met1606	9.5	20	20	0	NS
Met1521	6.9	30	0	10	NS
Met1761	6.4	40	30	20	P < 0.05
Met1860	14.4	20	20	20	NS

Methionine oxidation of VWF was measured using mass spectrometry. *The values indicate the percentages of patients whose oxidized methionine-to-total methionine ratio was greater than 1 at indicated time points (i.e., a higher level of methionine oxidation). Red: methionine residue at the ADAMTS-13 cleavage site, # Chi-Square test (χ^2), and NS: none significant.

SUPPLEMENTARY FIGURES

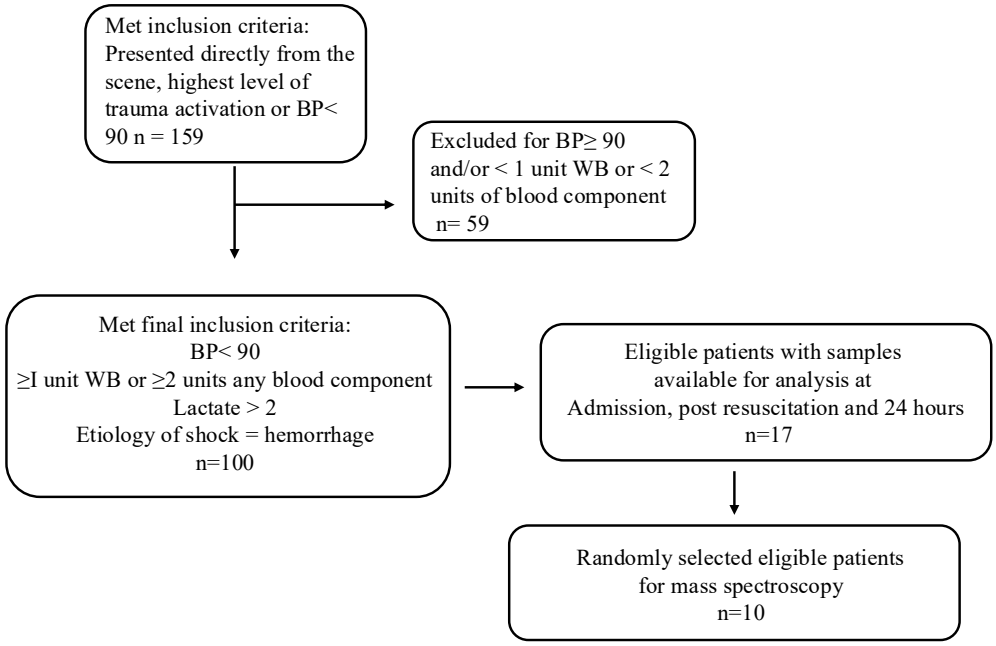

Figure S1: Schematic illustration of the study design. BP= blood pressure; WB= whole blood

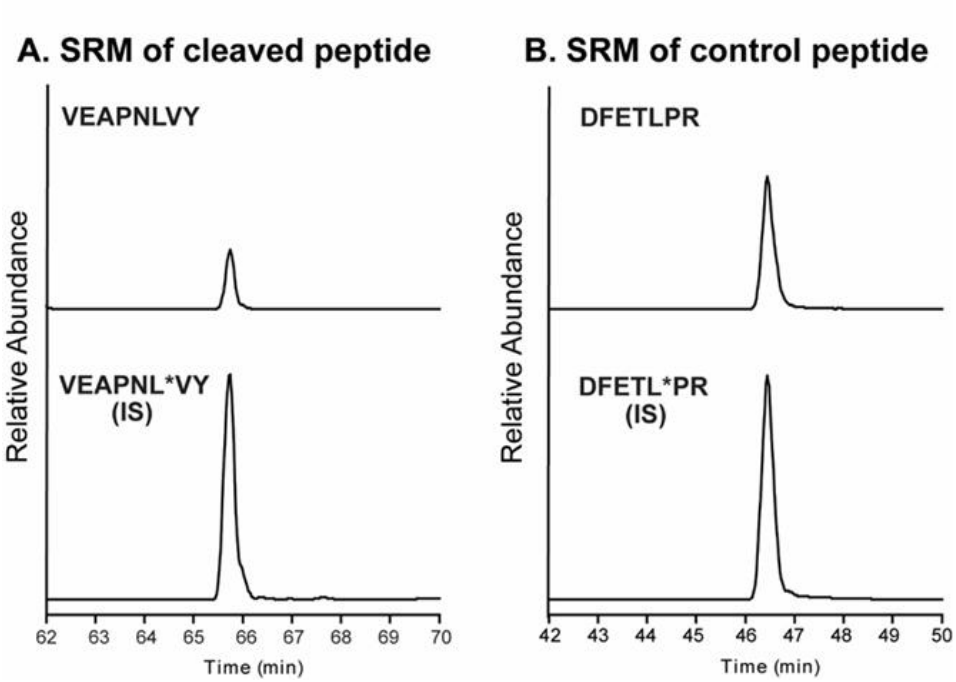

Figure S2: System setup for detecting ADAMTS-13 cleaved VWF in mouse plasma. Representative mass spectrometry profiles of selected reaction monitoring of ADAMTS-13-cleaved mouse VWF tryptic peptide VEAPNLVY. The tryptic peptide DFETLPR from the A2 domain was used as control to calculate the rate of VWF cleavage. Isotope-labelled peptides VEAPNL*VY and DFETL*PR (L*: U-13C615NL) were added as internal standards (IS) to quantify VWF and its cleavage. The VWF sequence flanking the ADAMTS-13 cleavage site: uncleaved tryptic peptide (underline: cleavage site): VEAPNLVYMVTGNPASDEIK Cleaved tryptic peptide: VEAPNLVY. **Abbreviation**: SRM: Selected Reaction Monitoring.

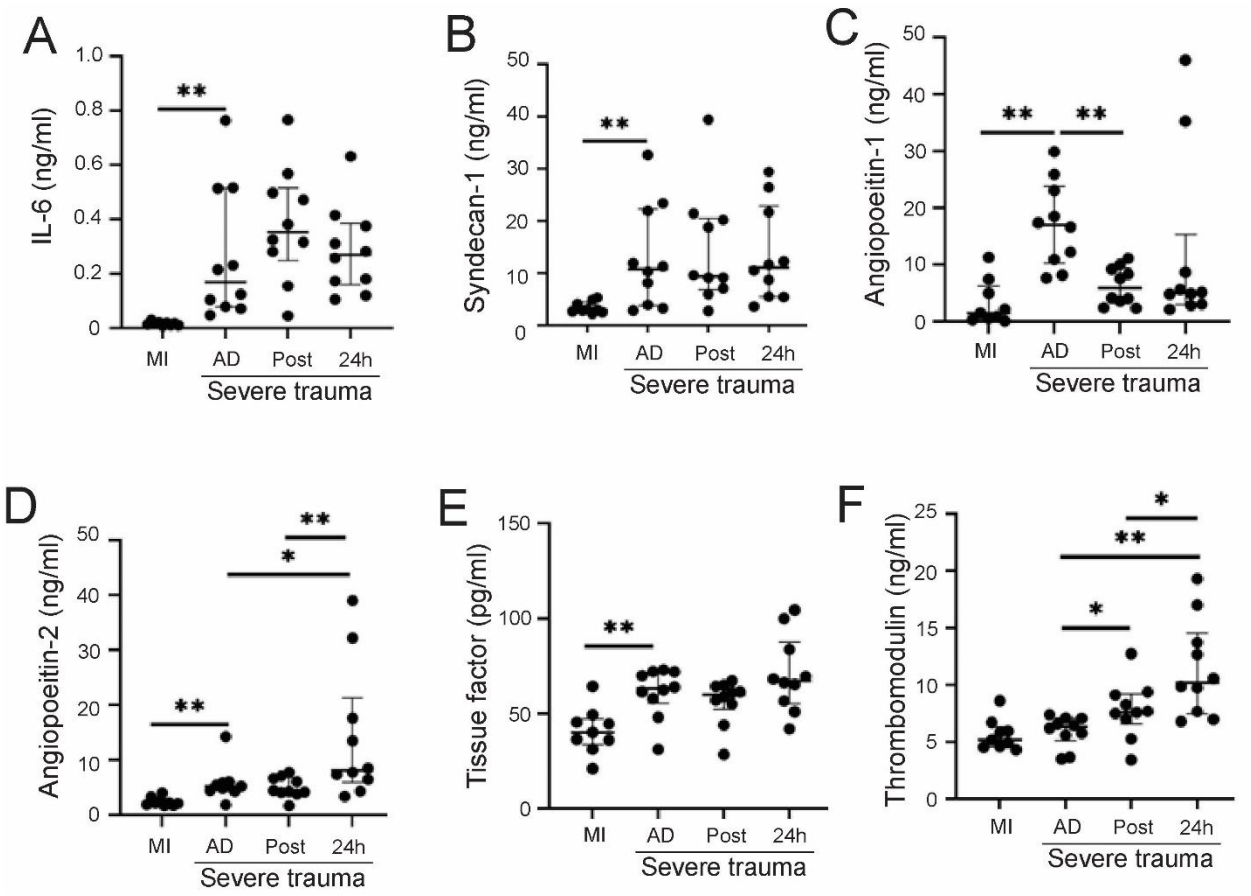

Figure S3: Longitudinal changes in markers of inflammation, endothelial injury, and coagulopathy in a subset of hemorrhagic shock patients. (A) IL-6 (B) syndecan-1 (C) angiopoietin-1 (D) angiopoietin-2 (E) tissue factor and (F) thrombomodulin. * $p<0.05$, ** $p<0.001$; data analyzed using Kruskal-Wallis one way analysis of variance on ranks. **Abbreviation**: MI: minimally injured; for severe trauma patients, AD: time of admission; post: post resuscitation and 24 hr: sample collected at 24 hours after admission.

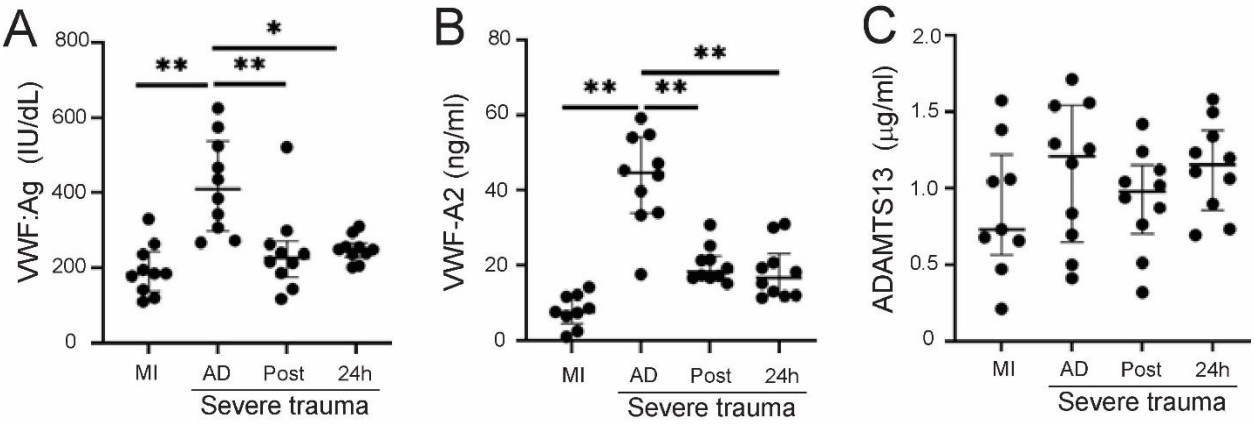

Figure S4: Longitudinal changes in hemorrhagic shock patients. (A) VWF antigen (Ag), (B) VWF-A2 and (C) ADAMTS13. * $p<0.05$, ** $p<0.001$; data analyzed using Kruskal-Wallis one way analysis of variance on ranks. **Abbreviation**: MI=minimally injured; for severe trauma patients, AD= time of admission; post= post resuscitation and 24 h=24 hours after admission.

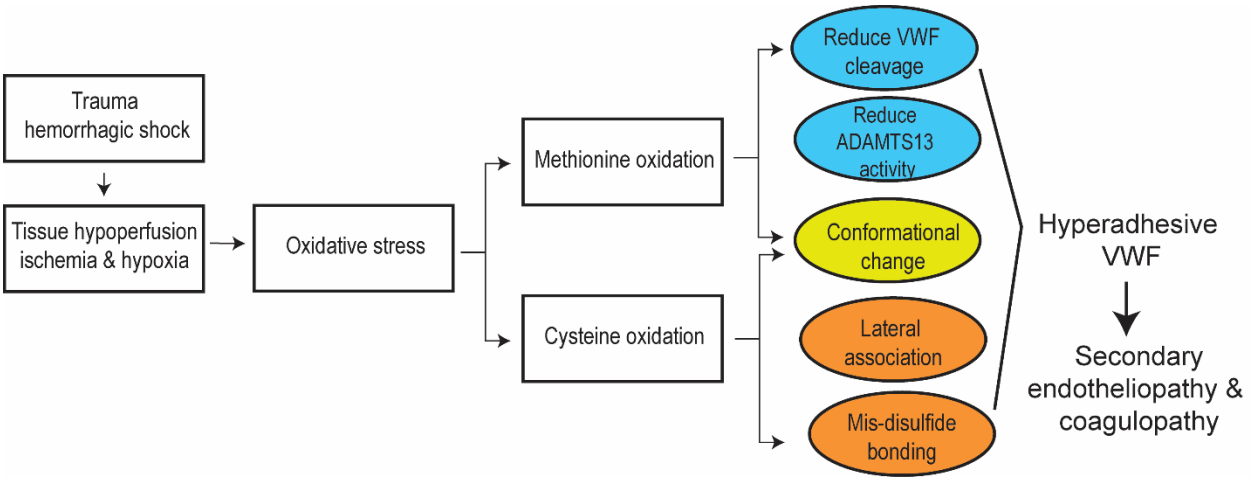

Figure S5: Schematic illustration of how oxidative stress causes changes in ADAMTS13-VWF axis, leading to the accumulation of hyperadhesive VWF that causes secondary endotheliopathy and coagulopathy.

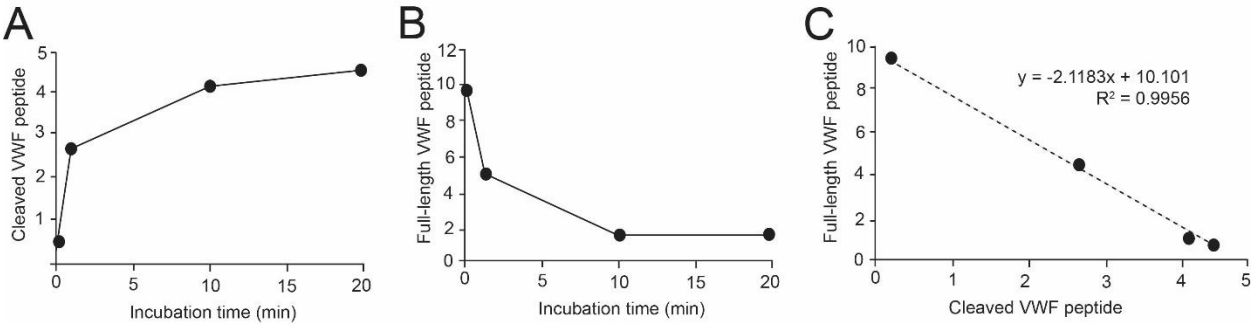

Figure S6: Cleavage of mouse VWF A2 by rhADAMTS-13. Mouse A2 (8.7 µg) was incubated with 10 ng of rhADAMTS-13 at 37ºC for 1, 10, and 20 min (A2 only as time 0). The cleavage was induced in the absence of urea and barium, but the HEPES buffer contained 2 mM of $CaCl_2$.